NBI and HHFW Fast Ion Temporal Dynamics Modeling with CQL3D-Hybrid-FOW in NSTX Discharges

R.W. Harvey, Yu. V. Petrov (CompX), D. Liu, W.W. Heidbrink (UCI), G. Taylor (PPPL), P.T. Bonoli (MIT)

Poster PP8.00079, APS/DPP Meeting, Oct. 27-31, New Orleans, LA

- The Fast Ion Diagnostic FIDA signal resulting from NBI and HHFW injected into NSTX has been simulated with the CQL3D Fokker-Planck, GENRAY, and FIDAsim codes.
- We report FIDA results from simulations with increasing fidelity to the expt, with ZOW, 1st-order orbit correction, FOW-hybrid.
- The FIDA experiment consists of a 1.0 MW modulated NBI with 0.4 duty factor, 0.020 sec total period (8 msec on, 12 msec off) for 11 periods. HHFW is on for a portion of the NBI beam blips, FIDA avg'd over 4 beam blips, as shown below in this slide.
- Plasma profiles evolve throughout:
  ne0=2.14 ==> 3.67e13, Teo=760 ==> 790, Tio=790 ==> 1190,
  Zeff=2.6 ==> 4.0, V_phi=80e3 ==> 100e3 rad/sec. (makes difference to NBI dep.)
- NBI and HHFW powers as below. FIDA signal obtained from last 4 beam-on periods.

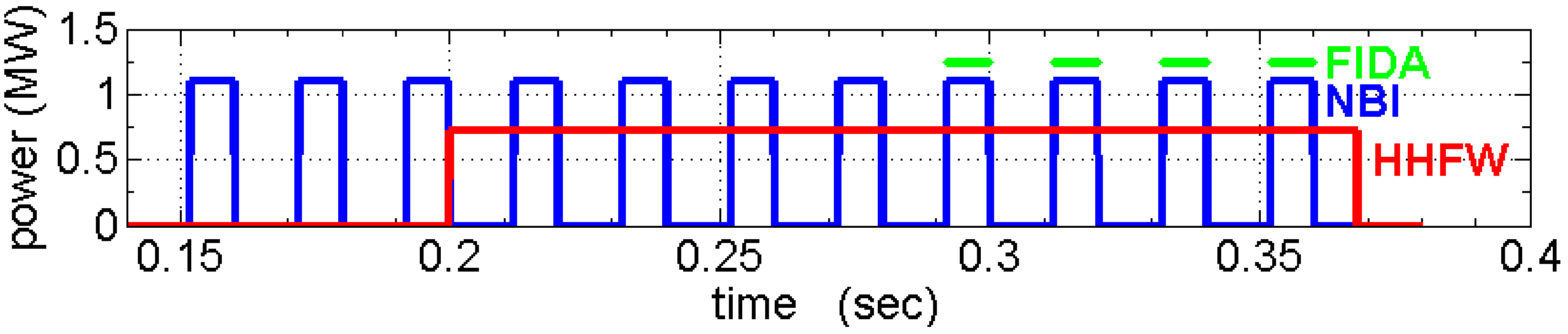

The Essence of Full-FOW:

We write the FPE in canonical action-angle ($\boldsymbol{J}, \boldsymbol{\Theta}$) space, then average over periodic angles.

$$\frac{\partial f}{\partial t}+\frac{d\boldsymbol{\Theta}}{dt}\cdot\frac{\partial f}{\partial\boldsymbol{\Theta}} = -\frac{\partial}{\partial\boldsymbol{u}}\cdot\boldsymbol{\Gamma}(f) = -\frac{\partial}{\partial\boldsymbol{J}}\cdot\left(\boldsymbol{\Gamma}\cdot\frac{\partial\boldsymbol{J}}{\partial\boldsymbol{u}}\right)-\frac{\partial}{\partial\boldsymbol{\Theta}}\cdot\left(\boldsymbol{\Gamma}\cdot\frac{\partial\boldsymbol{\Theta}}{\partial\boldsymbol{u}}\right)$$

where the collision (and QL) terms are expressed as divergence of a flux:

$$C(f)=-\frac{\partial}{\partial\boldsymbol{u}}\cdot\boldsymbol{\Gamma}(f)=-\frac{\partial}{\partial\boldsymbol{J}}\cdot\left(\boldsymbol{\Gamma}\cdot\frac{\partial\boldsymbol{J}}{\partial\boldsymbol{u}}\right)-\frac{\partial}{\partial\boldsymbol{\Theta}}\cdot\left(\boldsymbol{\Gamma}\cdot\frac{\partial\boldsymbol{\Theta}}{\partial\boldsymbol{u}}\right)$$

After bounce-averaging:

$$\langle C(f_0)\rangle=-\frac{\partial}{\partial\boldsymbol{J}}\cdot\left\langle\boldsymbol{\Gamma}(f_0)\cdot\frac{\partial\boldsymbol{J}}{\partial\boldsymbol{u}}\right\rangle$$

or

$$\langle C(f_0)\rangle=\frac{\partial}{\partial\boldsymbol{J}}\cdot\left(\underline{\underline{\boldsymbol{D}}}\cdot\frac{\partial}{\partial\boldsymbol{J}}f_0+\boldsymbol{F}f_0\right)$$

$$\underline{\underline{\boldsymbol{D}}}=\left\langle\frac{\partial\boldsymbol{J}}{\partial\boldsymbol{u}}\cdot\boldsymbol{D}^{\mathrm{uu}}\cdot\frac{\partial\boldsymbol{J}}{\partial\boldsymbol{u}}\right\rangle$$

$\boldsymbol{D}^{\mathrm{uu}}$ is the local diff. coeff. along orbit

$$\boldsymbol{F}=\left\langle\frac{\partial\boldsymbol{J}}{\partial\boldsymbol{u}}\cdot\boldsymbol{F}^{\mathrm{u}}\right\rangle$$

$\boldsymbol{F}^{\mathrm{u}}$ is the local friction coeff. along orbit

After transformation to a "convenient" set of I:

$$\Im \frac{\partial f_0}{\partial t} = \frac{\partial}{\partial I_i} \Im \left(\langle \frac{\partial I_i}{\partial \boldsymbol{u}} \boldsymbol{D}^{\mathbf{uu}} \frac{\partial I_j}{\partial \boldsymbol{u}} \rangle \frac{\partial}{\partial I_j} - \langle \frac{\partial I_i}{\partial \boldsymbol{u}} \boldsymbol{F}^{\mathbf{u}} \rangle \right) f_0$$

$$\Im = \left| \frac{\partial \boldsymbol{J}}{\partial \boldsymbol{I}} \right|$$ is the Jacobian of the transformation. Summation over i and j.

Choice of $\boldsymbol{I}$ space:

Computational grid: midplane R coord (R_0), u_0, pitch-angle at midplane (θ_0). A set of orbits with ($u_{0,j}$, $\theta_{0,i}$) launched from every R_0 grid point, and used for bounce-averaging of coll. operator and setting the loss cone).

Transformation from canonical action-angle space to the computational space, with averaging over gyro and bounce periods + tor.symmetry results in appearance of neoclassical radial transport terms.

In Hybrid-FOW, the FPE is in its original-ZOW form, with only two transformation coefficients retained $\left(\partial u_0 / \partial u = 1 \ , \ \partial \theta_0 / \partial \theta = \left(B_0 \sin\theta \cos\theta\right) / \left(B \sin\theta_0 \cos\theta_0\right) \ \right)$
But the mapping of particle and heat sources from the local off-midplane points to the midplane grid points is done along <Ψ_{pol}> of FOW orbits.

CQL3D Finite-Orbit-Width extension: Hybrid-FOW and Full-FOW models

Hybrid-FOW (used in this presentation)

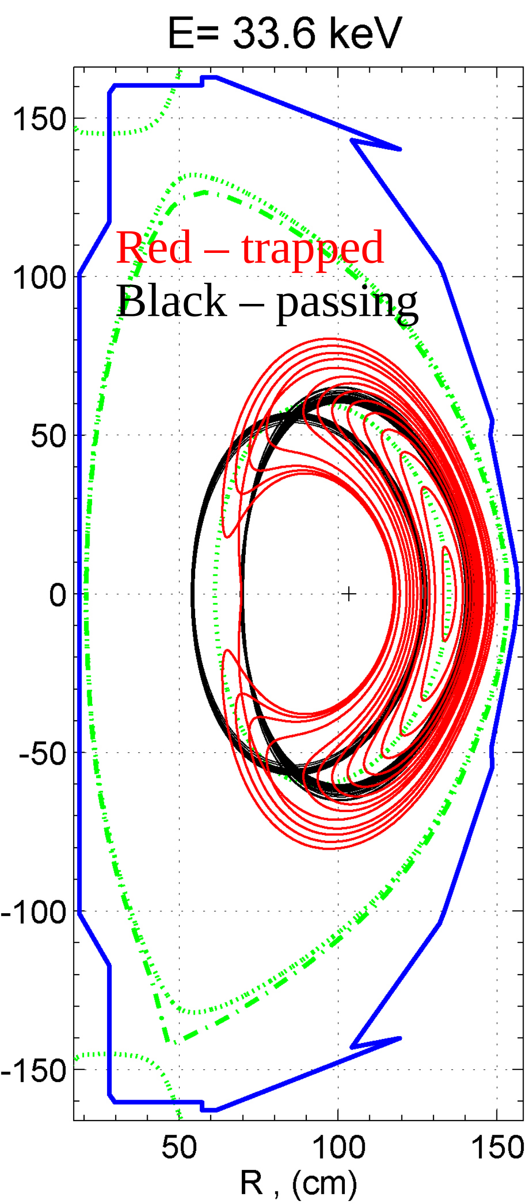

Distr. function for a given Ψ_{pol} consists of all orbits that have same $<\Psi_{pol}> = \Psi_{pol}$. **But the local *f* can be reconstructed from solution.**

Main Advantage:
Fast (only twice slower than ZOW)

Disadvantages:
- Only partial FOW capabilities (NBI, RF, diagnostics, loss cone).
- Collisions remain ZOW.
- No neoclassical transport (only model transport as in ZOW)

Full-FOW (in development)

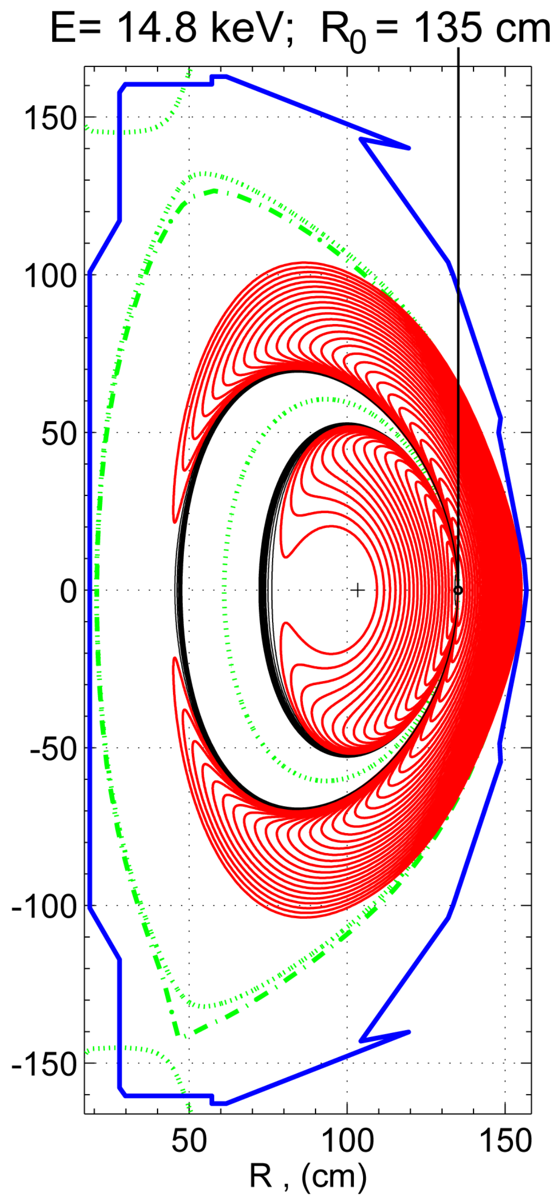

Actual local *f* at given R_0 at the midplane - made of all orbits that pass through R_0 ("0" refers to points on the midplane).

Main Advantage:
Neoclassical radial transport (ion radial transport ~ near neoclassical values in JET and DIIID, and probably ITER)

Disadvantages:
- Factor of 1000 slower than Hybrid-FOW (because of collisional operator, BUT parallelizable with good scaling).
- Complicated bndry conditions.

A Fast Look-up Table is Constructed Which Maps $(E, \mu, p_\phi) \rightarrow (R, u, \theta)_{midplane}$

For each (i_u, i_μ, i_{p_ϕ})-index, the values are stored:

1. R_0-coordinates of orbit "legs" on the midplane.
2. Similarly, $\cos\theta_0 \equiv (u_{||}/u)_0$ values.
3. Ψ_{pol}-values at orbit "legs" on the midplane.
4. $<\Psi_{pol}>$ and τ_b : found from g.c. orbit tracing.

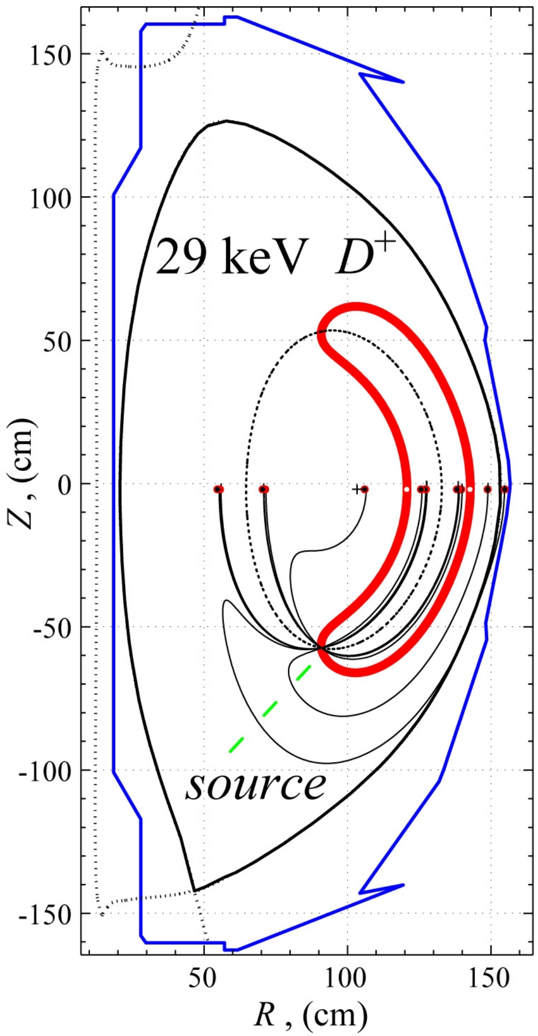

Used for:

1. Formation of Source operator, in terms of midplane grids.
2. RF QL operator.
3. Reconstruction of local f along the sight-lines.

←Thin lines are from g.c. orbit tracing. Dots on the midplane are from the Look-up Table. In the **Hybrid-FOW** model, the red orbit is attributed to the dashed flux surface $\Psi_{pol} = <\Psi_{pol}>$

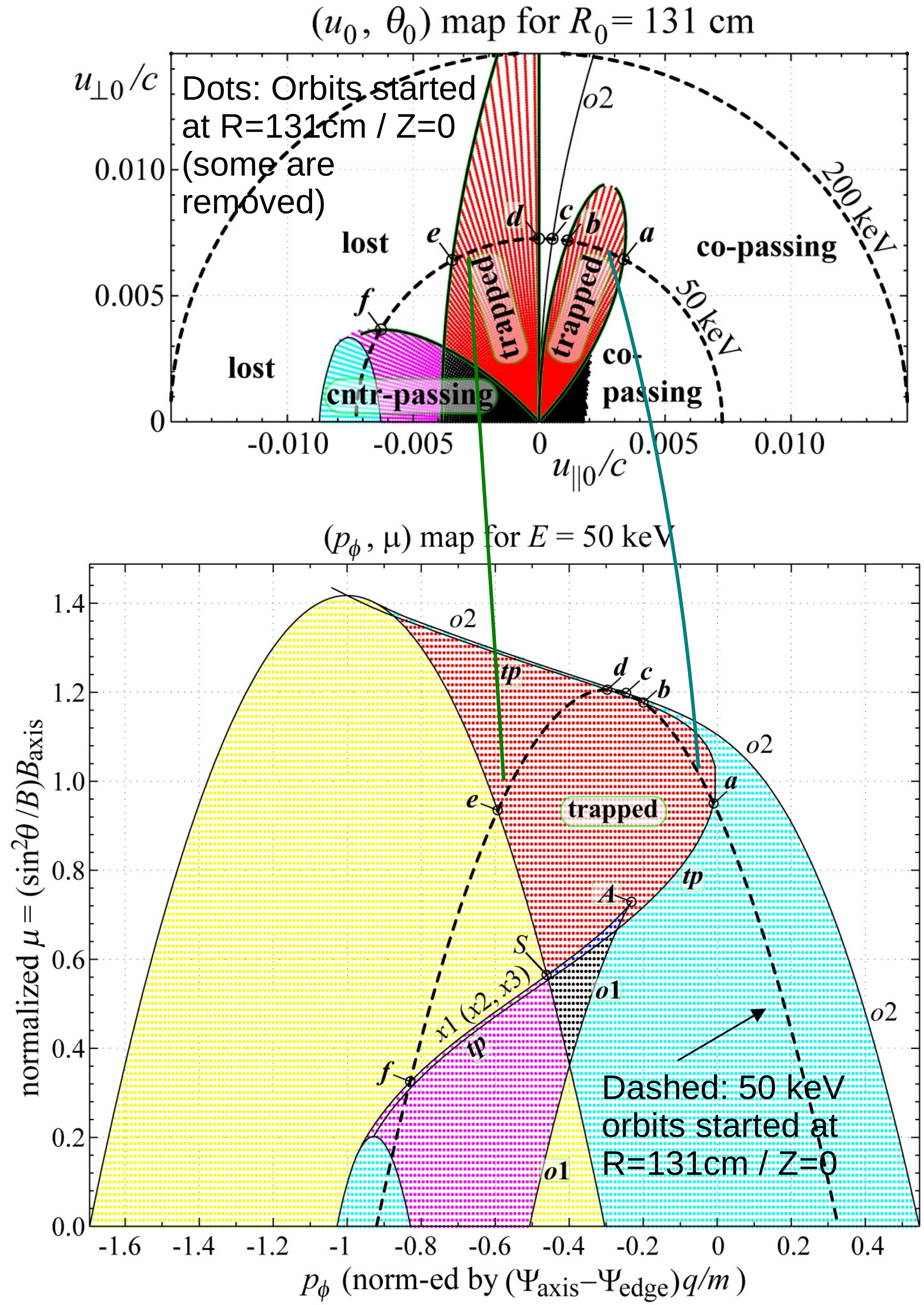

Hybrid-FOW

How to Reconstruct Local Distribution Function – needed for diagnostics

Method: Mapping the Constants of Motion (COM) space of energy, adiabatic invariant and canonical toroidal momentum $(E,\, \mu,\, p_{\phi})$ onto the midplane values $(u_0\,,\ \theta_0\,,\, R_0)$ where the grids are defined.

1. Consider point $(R,\, Z)$ and a particle with local (u,θ).
2. Evaluate $(u,\, \mu,\, p_{\phi}\ )$.
3. Find the nearest $(i_u\,,\, i_{\mu}\ ,\ \ i_{p_{\phi}})$ index in the Look-up Table; identify proper orbit.
4. Find the value of $<\Psi_{\rm pol}>$ from the Table – then, determine the two nearest FP'd surfaces; use interpolation to calculate the value of *local* $f(R,\, Z,\, u,\theta)$.

Solution ($f_{soln} = f_{BA}$) | Local f (reconstructed)

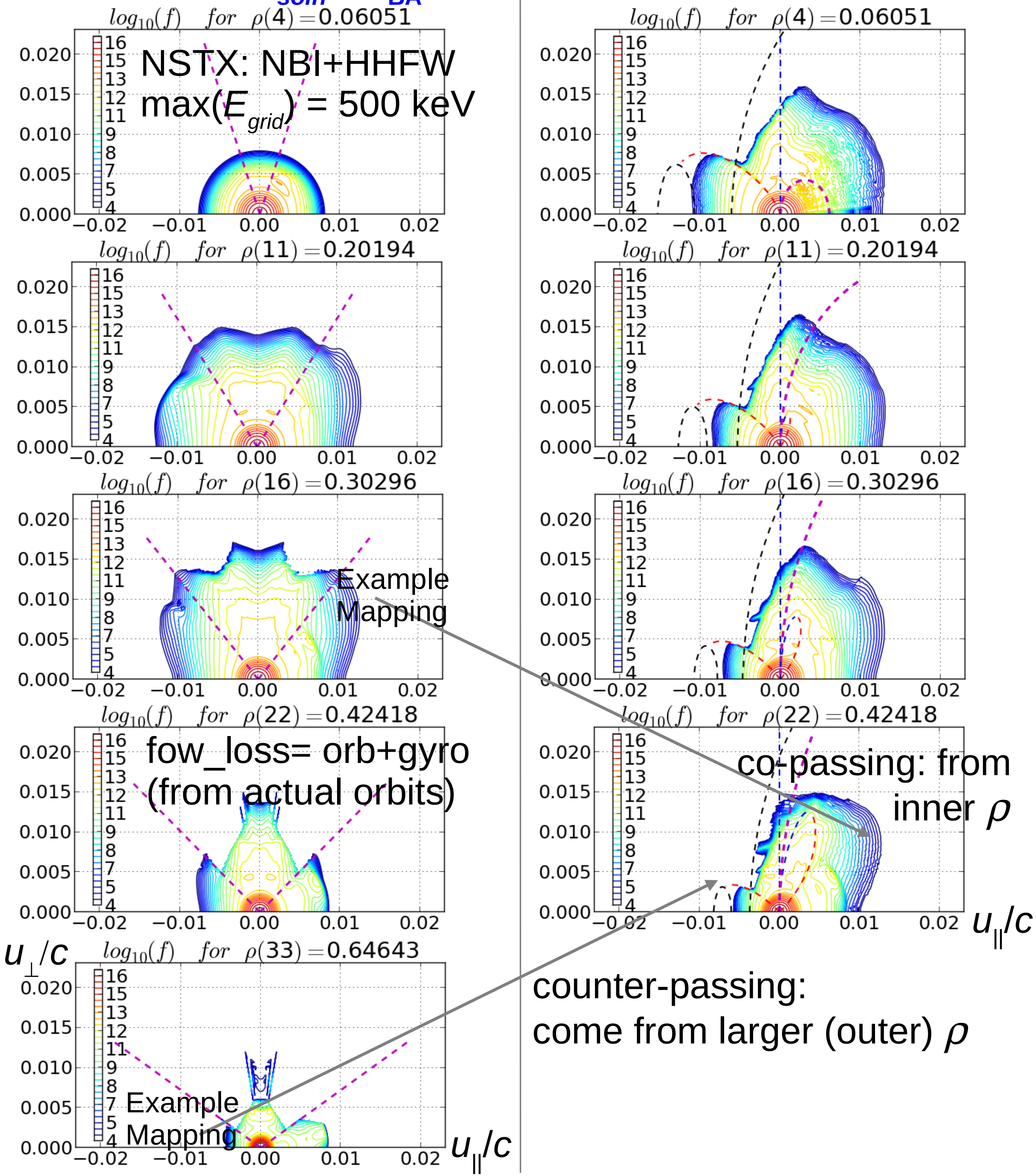

Experimental Traces for NB/HHFW Power, Elec Density and Temperature, MHD Mode Activity, and Neutron Rates from NBI, With/Without HHFW

NSTX NBI+HHFW Shot 12879
NBI only, No HHRW, Shot 123742

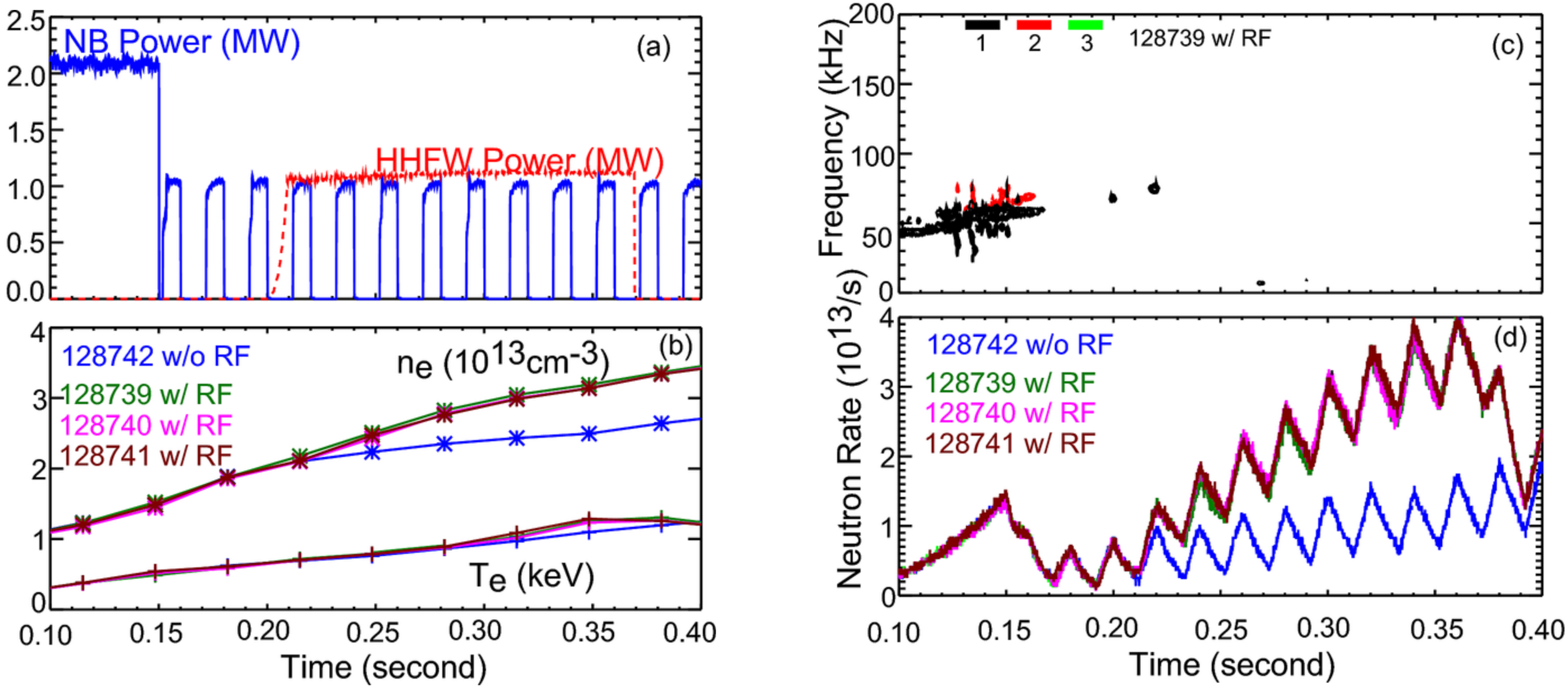

The RF Data for NSTX High Harmonic Fast Wave Heating is Obtained with the GENRAY Ray Tracing Code, Thereby Calculating the QL Diffusion Coefficients Used in the CQL3D FP Code

- GENRAY [compxco.com/genray] solves the usual ray tracing equations for trajectories and ray characteristics (kpar, kperp, polarizations, energy flux factor), for the 30 MHz HHFW, RF energy injected into NSTX. Cyclotron harmonics range 2-11 Ω_{cD}.
- Considering the ray trajectories to consist of short ray elements occupying a small spatial volume, the local RF diffusion coefficients are calculated using Stix-like (1992) expressions [compxco.com/cql3d]. These are bounce-averaged, providing diffusion contributions evaluated at the plasma midplane. Solution of the Fokker-Planck equation at each radius gives the nonthermal BA distribution functions.
- Power absorption at each ray element along the trajectory is calculated self-consistently with the nonthermal distributions, as $\int d^3u(1/2)mv^2\partial f/\partial t|_{QL}$, evaluated from the BA distns.

Ray Trajectories

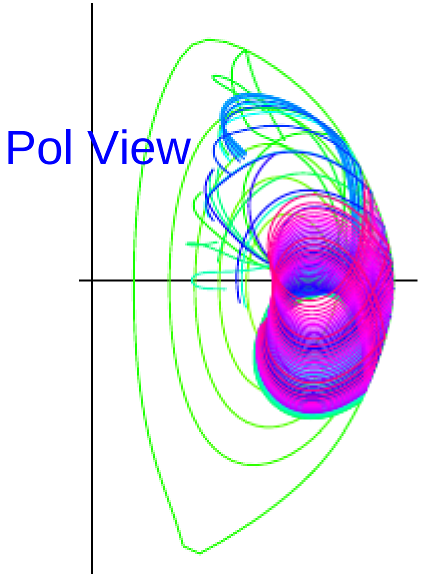

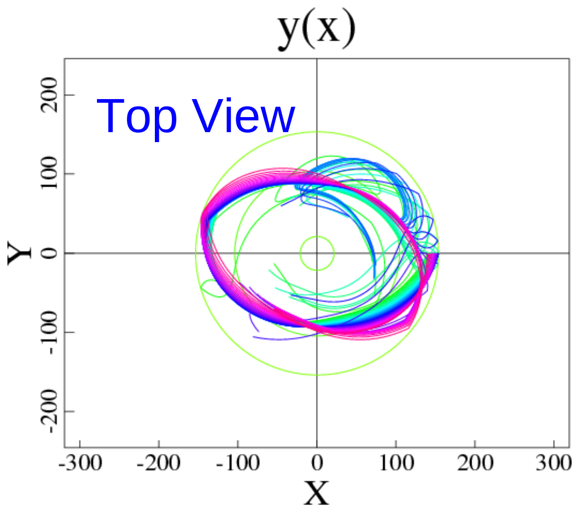

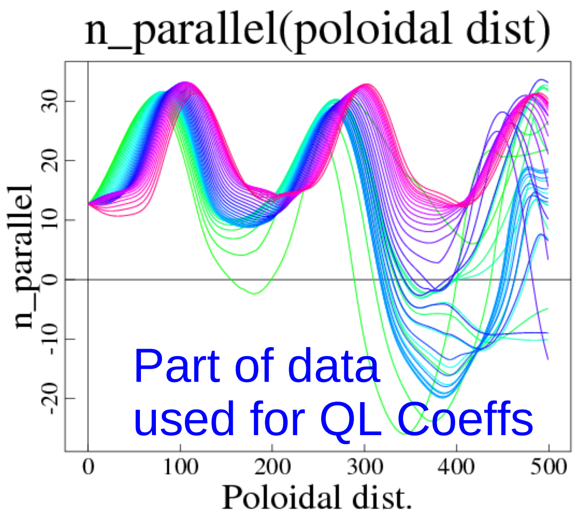

Liu *et al.* Comparison of CQL3D with FIDA, 2008-2010

- Deyong Liu (w Heidbrink) compared NSTX FIDA results with several simulations, as below (Liu et al., PPCF, 2010).
- TRANSP and ORBIT-RF agreed with experimental FIDA signal radial profile much better than zero-orbit-width (ZOW) CQL3D.
- TRANSP did very well for NBI, but did not have HHFW capabilty.
- CQL3D/FIDA was shifted inwards in minor radius relative to experiment (below).
- Liu et al. and Choi et al. attributed CQL3D problem to ZOW.
- Therefore, began finite-orbit-width extension (FOW) of CQL3D.

Plasma Phys. Control. Fusion **52** (2010) 025006 D Liu *et al*

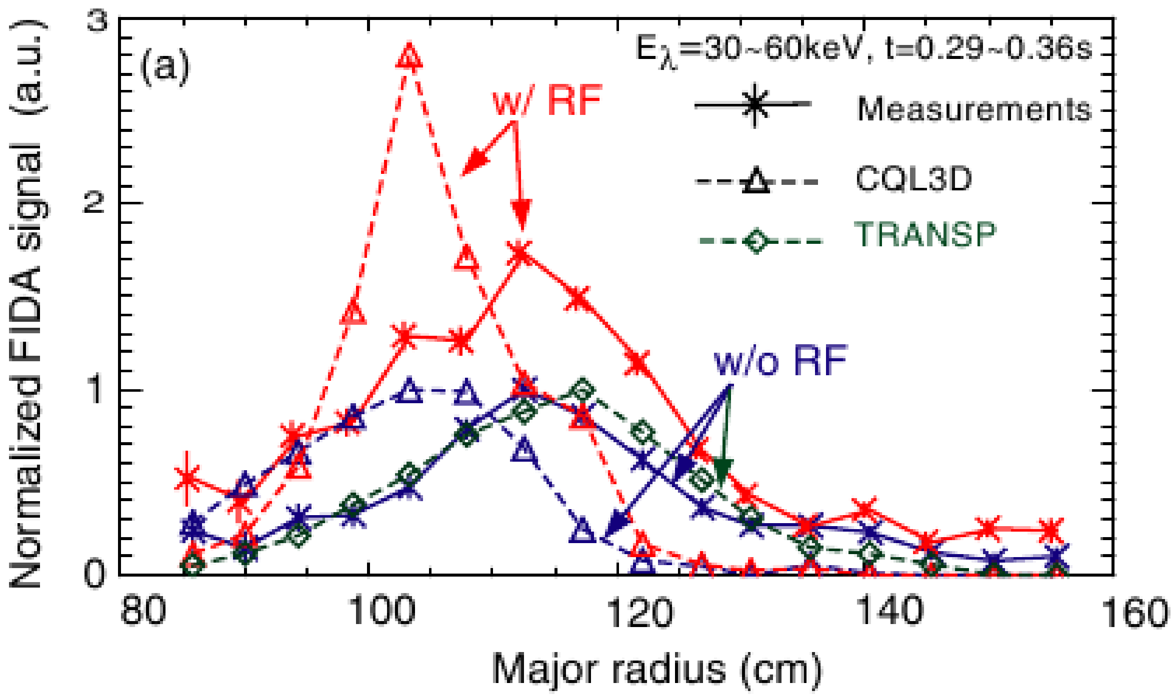

FIDA Calcs with Improving CQL3D Models (+ FIDAsim code)

Spline-time-dependent plasma profiles added to CQL3D. Using TRANSP/exptl profiles.

NBI: FIDA/CQL3D calcs normalized to experimental peak. ZOW shifted inwards, 1^{St} -order orbit correction in CQL3D greatly overestimates R-shift. Hybrid-FOW gets peak close to expt. but width a little too great.

NBI+HHFW: Simlar problem with ZOW and 1^{st} -order, but Hybrid-FOW good.
==> Good agreement with HHFW peak (adjusted only for canonical 35 % edge loss. Provides additional confirmation of 35% edge losses.)

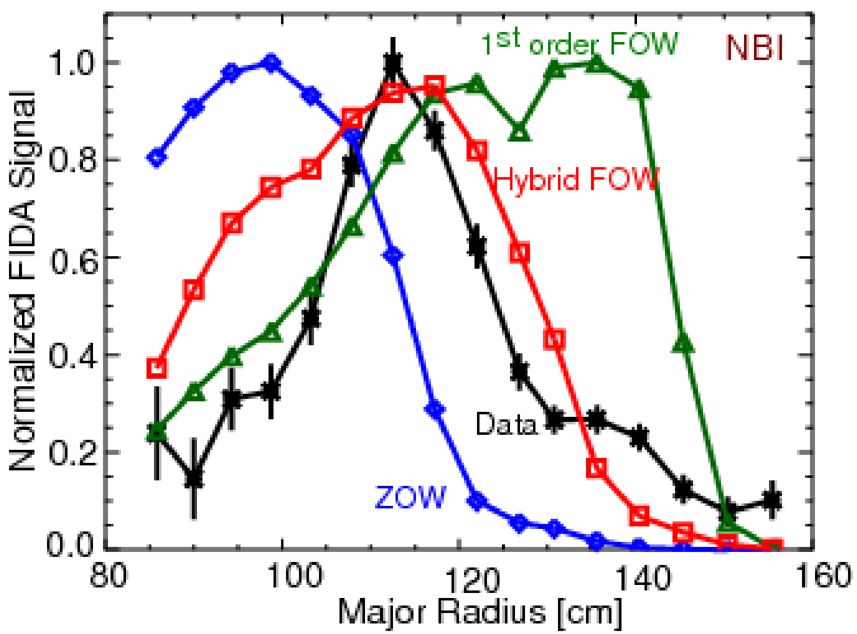

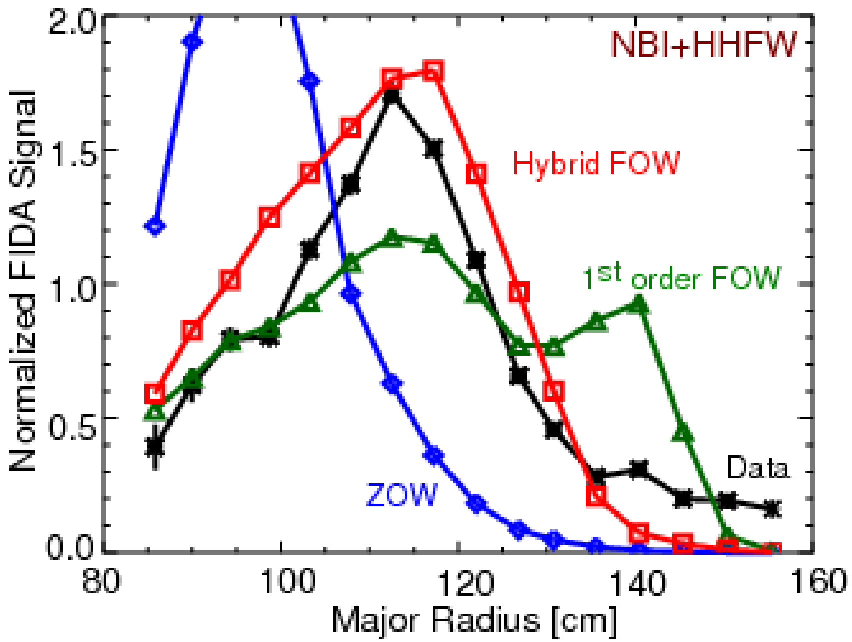

GOOD AGREEMENT OF SIMULATED AND EXPERIMENTAL ENERGY SPECTRA FOR FIDA AND NPA

FIDA | NPA

NBI

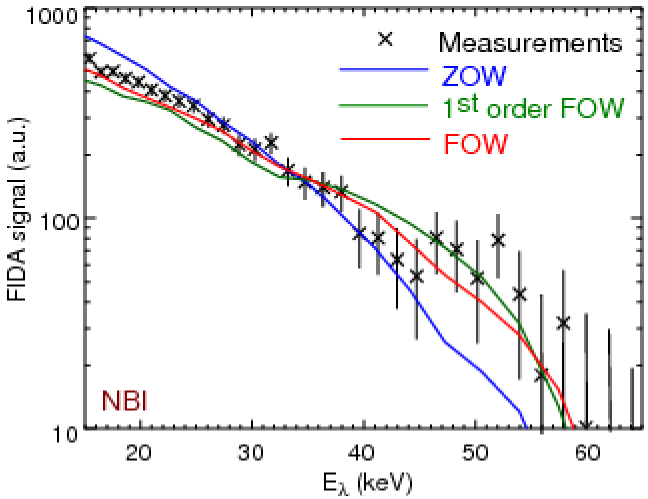

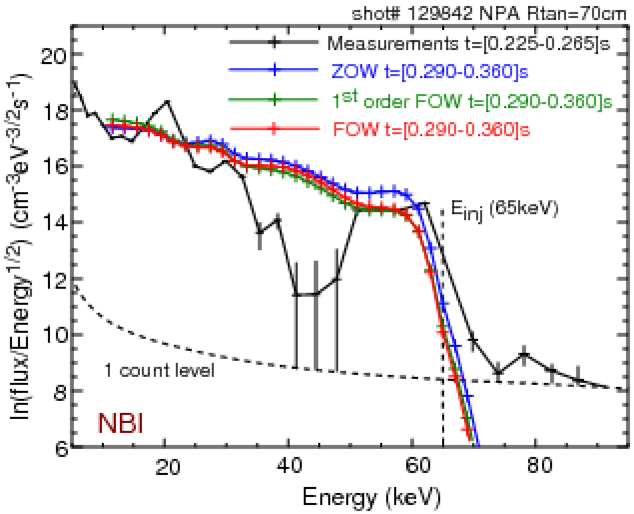

NBI+HHFW

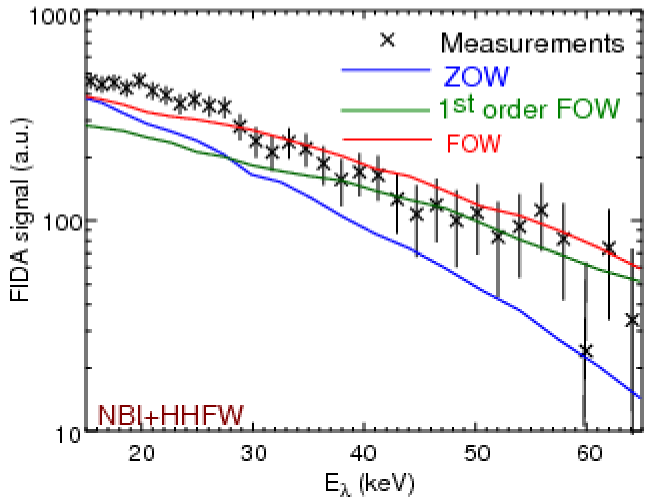

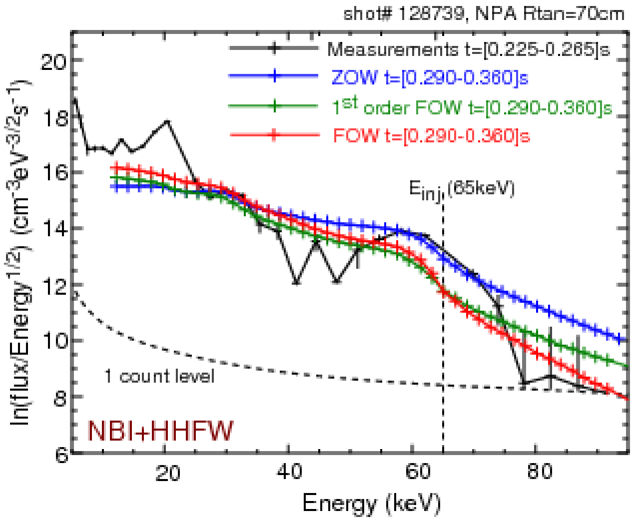

NPA as a Function of Energy and Time Tests Several Time Scales

In general, all synthetic diagnostics can be calculated from the distributions functions. Time dependent diagnostics, NPA for example here, contain a wealth of testable plasma information.

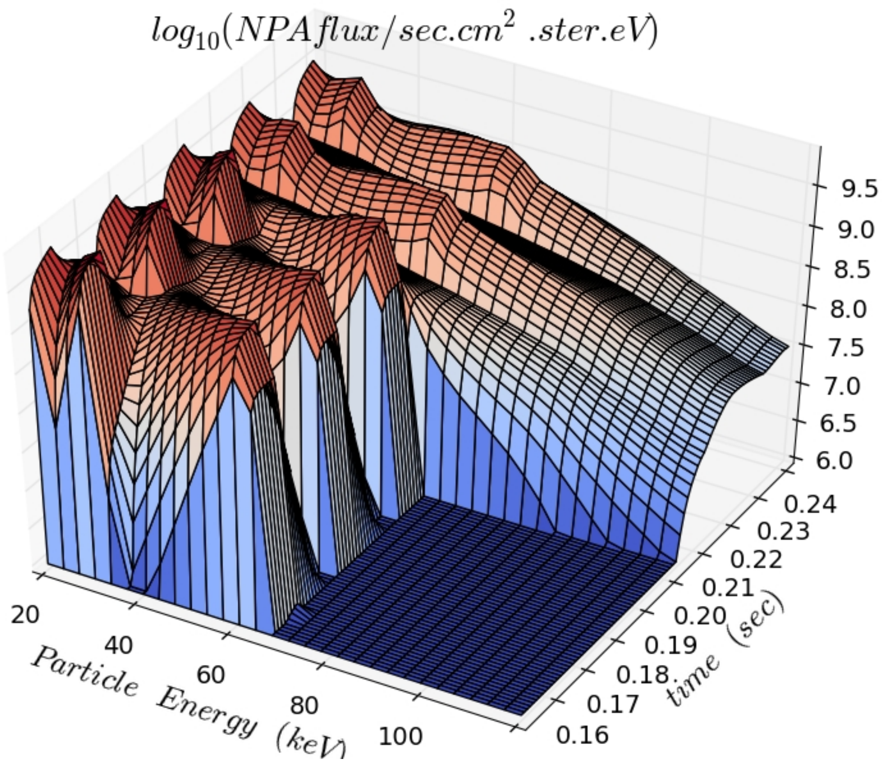

Beam blips (8 msec on, 12 msec off) give:

- Heating times due to NBI source heating, indicated by NPA rampup.
- QL diffusion and heating rates due to HHFW
- Collisional FI slowing indicated by development of NPA at energies below the NB inj. energies, and by NBI turnoff.

Good Simulation/Experiment Agreement, Becoming Less at Late Times

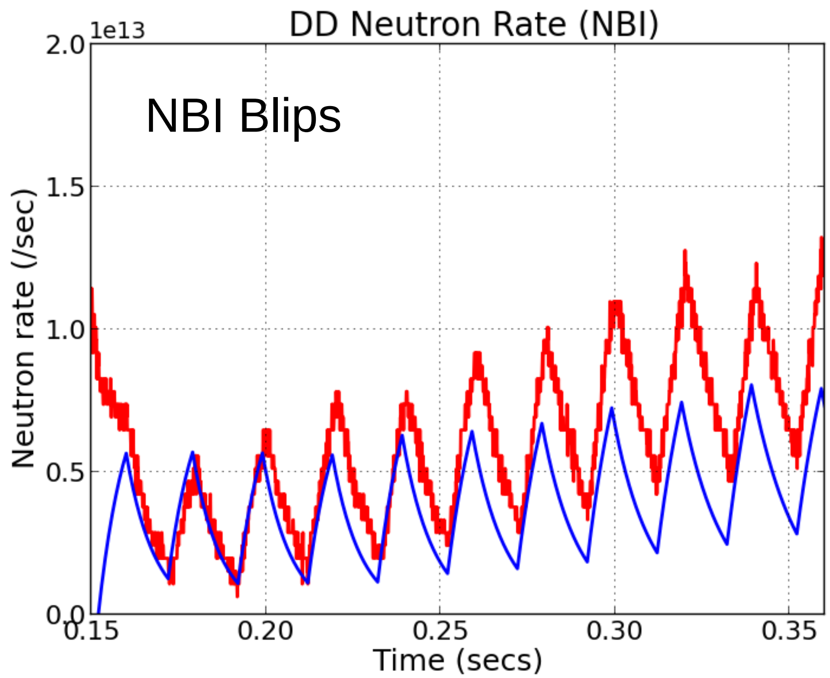

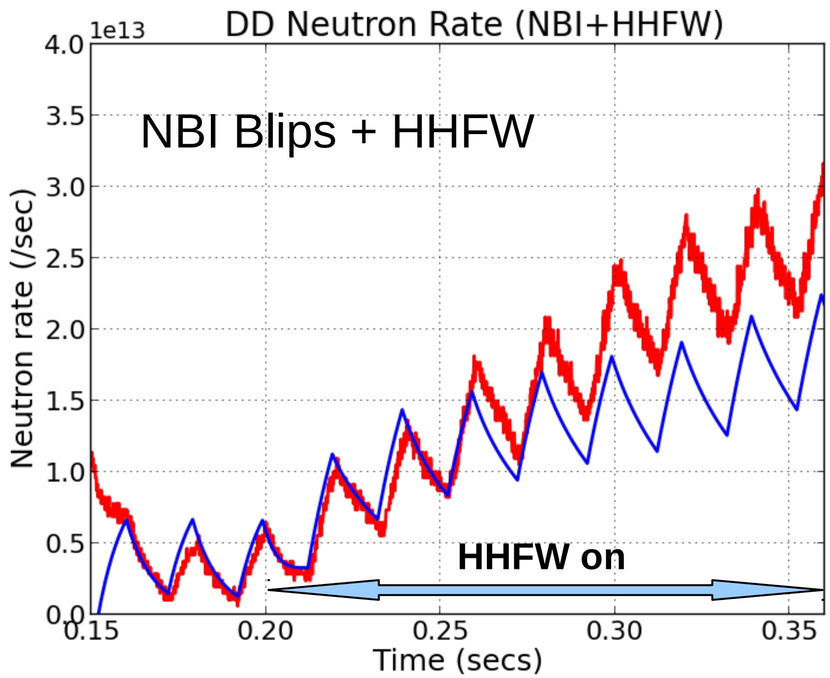

Conjecture:

D^+ distribution function calculation includes CX losses, with background neutrals calculated with FRANTIC, flux-surface based code (2-3D model would be better).
==> Will examine possibility that neutrals' CX effect is too high at late times.

FI Losses are Substantially Increased by HHFW, Compared to NBI

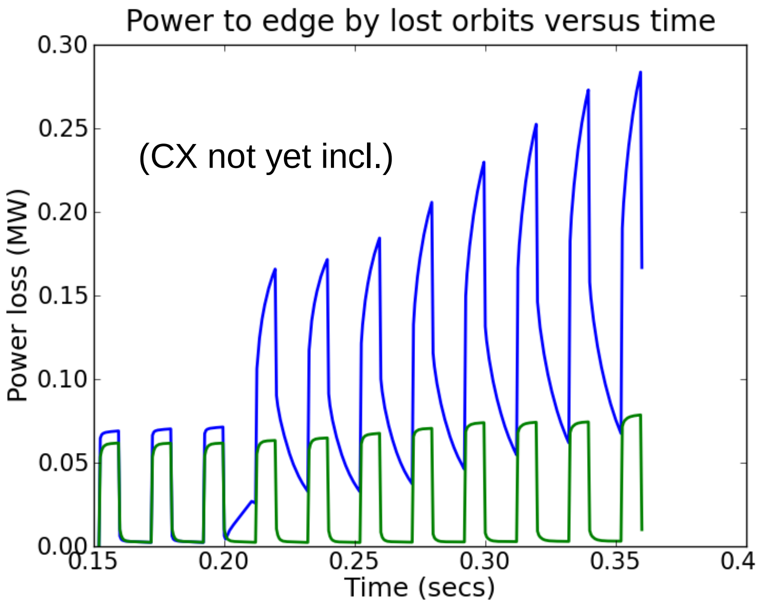

NBI phase: 7% loss (0.07 out of 1.0 MW input) lost to wall

NBI+HHFW: Additional 14-28% loss (0.1-0.2 MW out of 0.71 MW input) lost

Explanation: NBI injected into low loss region of velocity space.
HHFW spreads FIs into loss cone (which exists at all radii, as shown below).

Radial profile of FI loss power versus time (0.0 – 0.1 W/cm^3)

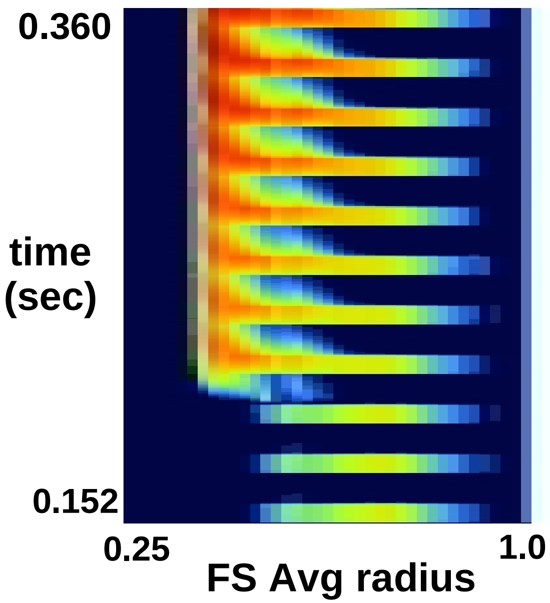

Loss Bndry in local vel space, at each radius

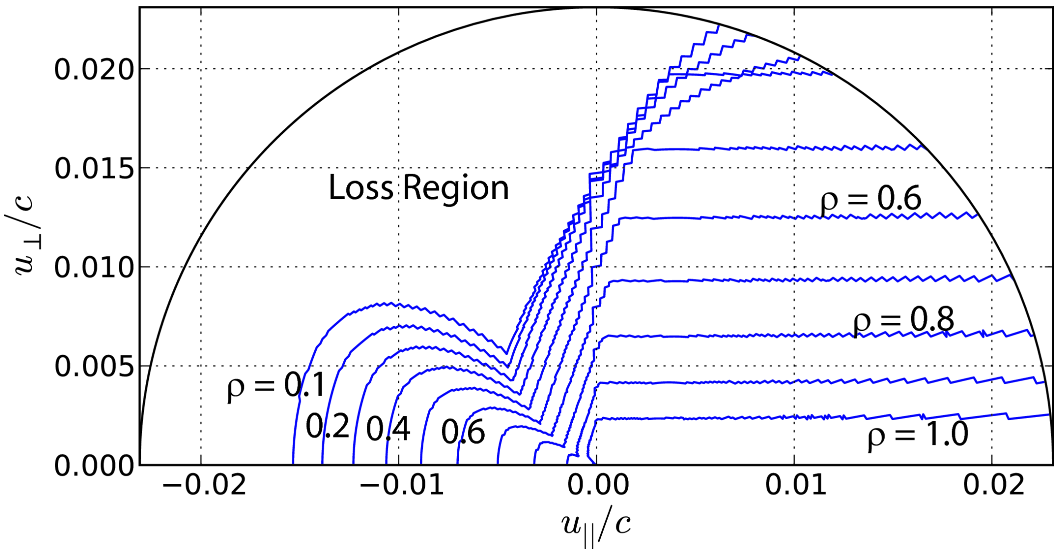

CONCLUSIONS

- Successive refinement of CQL3D, particularly addition of FOW-HYBRID gives quite accurate FI distributions for NSTX FIDA (Calc'd with FIDAsim). This is determined from both spatial and energy spectra, and also for NPA. We hope that the full FOW neoclassical simulation in CQL3D (with radial diffusion) will result in improved agreement of FIDA toward the plasma periphery.

- HHFW substantially increases fast ion orbit losses, above those for NBI, due to scattering for ions into the loss regions. We will examine this in greater detail.

- Neutron rates are in general accord between simulation and experiment (per Deyong Liu and simulation of experimental signals).

- We have independent agreement with the typical assumption of ~30% losses of HHFW power near the plasma edge.

- Computer time for the simulations was up to 20 cpu hours (single core) for 20 msec time-dependent, modulated beam simulation. CQL3D is MPI'd over flux surfaces, which scale well when no radial transport. (Parallelized big matrix solver with radial transport is work in progress.)

- The smooth FOW distributions from the comprehensive time-dependent CQL3D Fokker-Planck code along with a range of synthetic diagnostics, provide a means for detailed investigation of the physics model.